Drag effect of steam flow on droplet removal during dropwise condensation at different surface inclinations

Journal of Physics: Conference Series **2766** (2024) 012133 doi:10.1088/1742-6596/2766/1/012133

Drag effect of steam flow on droplet removal during dropwise condensation at different surface inclinations

A Abbatecola, M Tancon, S Bortolin and D Del Col

University of Padova, Department of Industrial Engineering
Via Venezia 1, 35131 – Padova, Italy

E-mail: antonio.abbatecola@studenti.unipd.it

Abstract. Dropwise condensation is a quasi-cyclic process characterized by the nucleation, growth, and removal of discrete liquid droplets on a subcooled surface. The removal of condensate is a critical aspect, usually achieved by exploiting the gravity force, the drag force of vapor or the surface wettability gradient. This paper presents an experimental study of the vapor drag action on condensate removal, with focus on droplet's departing radius (r_{max}). Specifically, for the experimental campaign, vapor velocity was varied from 3 to 14 m s^{-1} considering three different surface inclinations: vertical, 45° inclined, and horizontal. The results showed that, as the velocity increases, the difference in departing radii among the three different configurations decreases and, consequently, the difference in heat transfer coefficients decreases too. In fact, at the highest vapor velocity (~14 m s^{-1}), r_{max} was almost equal for all the inclinations leading to similar heat transfer coefficients (~120 kW m^{-2} K^{-1}). Interestingly, on a horizontal surface considering vapor velocity equal to 3 m s^{-1}, despite the lack of gravity's contribution to droplet removal, no transition to filmwise condensation was observed.

1. Introduction

Dropwise condensation (DWC) is a complex two-phase heat transfer mechanism described as a quasi-cyclic process. Once the nucleation occurs, droplets grow by both direct condensation and coalescence until they reach the departing radius (r_{max}). The latter represents the maximum size attainable by a droplet before sliding along the surface, making new nucleation sites available [1].

The arising interest in DWC is related to its phenomenology, specifically to the presence of small droplets. Indeed, DWC avoids the formation of a continuous film of liquid between the condensing surface and the vapor that, becoming thick, penalizes the heat transfer. The promotion of DWC allows to obtain heat transfer coefficients (HTCs) 10 times higher than those achievable during filmwise condensation (FWC), providing both economic and energy benefits [2,3]. However, for efficiently promoting DWC on metals, low surface energy coatings are needed [4].

Over the years, several works in the literature have investigated DWC on vertical surfaces under quiescent vapor conditions, but only few have delved into the phenomenon investigating the effects of vapor velocity and surface inclination [5,6]. Nevertheless, understanding the influence of these parameters could be of great interest for future industrial applications. Therefore, the present study aims to fill these gaps by studying the effect of such parameters on condensate removal and heat transfer.

Typically, condensate removal occurs by means of gravity force. However, in the case of horizontal or slightly inclined surfaces, gravity may not be enough to remove the condensate, possibly leading to flooding of the surface and transition to FWC. In such cases, two alternative methodologies of droplet

removal can be exploited. The first relies on wettability gradients [7], while the second leverages the drag effect exerted by the flowing vapor on the condensing surface [5]. This study shows that vapor drag is an effective method for removing condensate, even on horizontally oriented condensing surfaces.

2. Experimental Methods

The experimental results presented in this paper were obtained using the setup described by Tancon et al. [8]. It consists of a thermosyphon loop where the vapor, generated in a boiling chamber, partially condenses in the test section by exchanging heat with a stream of cold water coming from a thermostatic bath. To complete the condensation process, the two-phase mixture exiting the test section is directed into a post-condenser. The cycle closes with the return of the condensate to the boiling chamber. A schematic representation of the layout is reported in figure 1a. It is worth mentioning that the test section was designed to allow simultaneous heat transfer measurements and DWC visualizations using high-speed imaging. As stated in the introduction, the analyses have been carried out by varying the condensing surface inclination (β) and the vapor velocity (v_{vap}). The piping system was designed to allow three different positions of the test section: vertical (figure 1b), 45° inclined (figure 1c), and horizontal (figure 1d). Regarding the vapor velocity, it has been varied from approximately 3 to 14 m s^{-1} by acting on the power of the boiling chamber. Throughout the experimental campaign, three samples were tested, one for each configuration. They consisted of aluminium substrates on which a low surface energy coating was deposited. One coating was fabricated by sol-gel technique using phenyl-triethoxy-silane and methyl-triethoxy-silane as precursors in a molar ratio of 70%-30% (this coating is named P7M3). An additional sample was tested in vertical configuration to assess the effect of surface wettability on DWC performances. In this case, the precursors used were octyl-triethoxy-silane and tetra-ethyl-orthosilicate in a molar ratio of 20%-80%, hereafter referred to O2T8. Further details about the coatings are reported in Parin et al. [9].

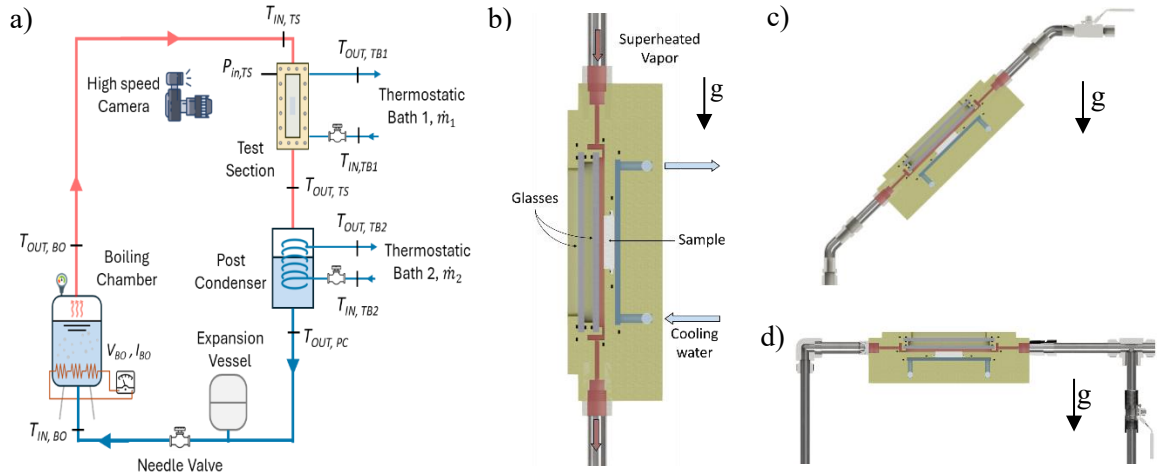

Figure 1. a) Layout of the experimental apparatus. Cross-sectional view of the test section in three different configurations: b) vertically oriented ($\beta = 90°$), c) 45° inclined ($\beta = 45°$) and d) horizontally oriented ($\beta = 0°$).

The wettability of the samples was characterized using the sessile drop method both before and after condensation tests. All the P7M3 samples exhibited similar wettability with advancing contact angle $\theta_a = 87° \pm 2°$ and receding contact angle $\theta_r = 64° \pm 5°$ before the tests. Thus, P7M3 samples can be considered as hydrophilic with a low contact angle hysteresis After tests, the same samples showed $\theta_a = 88° \pm 3°$ to and receding contact angles $\theta_r = 61° \pm 6°$. Regarding the O2T8 sample, it displayed a hydrophobic behaviour with $\theta_a = 101° \pm 2°$ and $\theta_r = 87° \pm 4°$ before the tests and $\theta_a = 97° \pm 3°$ and $\theta_r = 82° \pm 3°$after DWC measurements.

The focus of this study is on the droplet removal mechanism. Therefore, the parameters here investigated are the droplet departing radius (r_{max}) and the heat transfer coefficient (HTC). The departing

radii have been analysed by recording videos with a high-speed camera coupled with a LED source and a macro lens. Subsequently, videos have been post-processed with a homemade MATLAB® program, able to detect the droplets dimensions just before a sliding event. On the other hand, the HTC was evaluated according to equations 1,2 and 3 reported in table 1.

Table 1. Equations used for data reduction.

$$q = \frac{\dot{m}_{TB1} c_w \Delta T_w}{A} \quad (1)$$

$$\Delta T = \sum_{i=in}^{out} \frac{\left(T_{sat} - T_{surf,i}\right)}{3} \quad (2)$$

$$\mathrm{HTC} = \frac{q}{\Delta T} \quad (3)$$

$$v_{vap} = \frac{Q_{BC}}{\left(h_{vap} - h_{ls}\right) \rho_{vap} S_{ch}} \quad (4)$$

Equation 1 represents the thermal balance on the coolant side of the test section, aimed at calculating the average heat flux exchanged through the condensing surface. In this equation, $\dot{m}_{TB1}$ is the mass flowrate of the coolant water coming from the thermostatic bath 1, c_w is the water specific heat and ΔT_w is the cooling water temperature difference. Equation 2 is used to compute the saturation-to-wall temperature difference. Using thermocouples embedded in the sample and applying the Fourier's law is possible to evaluate the surface temperature at three different longitudinal positions along the sample. The saturation temperature is obtained by the readings of the saturation pressure at the inlet of the test section. Finally, as stated in equation 3, the ratio of heat flux obtained with equation 1 and the temperature difference given by equation 2 allows to evaluate the HTC.

Another parameter used in the present work is the vapor velocity (v_{vap}). The latter is evaluated by applying a thermal balance at the boiling chamber as shown in equation 4, where: Q_{BC} is the electrical power supplied to the boiling chamber, h_{vap} and h_{ls} are respectively the specific enthalpies of the subcooled liquid entering the boiling chamber and saturated vapor exiting the boiling chamber, ρ_{vap} is vapor density at the saturation pressure and S_{ch} is the cross sectional area of the vapor channel within the test section (5 mm × 30 mm).

Each experimental point presented in this paper was obtained as the average of 480 measurements taken at a frequency of 1 Hz. To ensure accurate heat transfer measurements, temperature transducers were calibrated: after calibration the accuracy of the thermocouples is ±0.05 K, while the thermopile has an accuracy of ±0.03 K. Further details about the calibration procedure are reported in Tancon et al. [8]. The main parameters underwent uncertainty analysis considering a coverage factor k = 2 for the evaluation of combined uncertainties. Table 2 shows the operating conditions for the tests and the combined uncertainties associated with the measurements.

Table 2. Summary of the operating conditions with combined uncertainties.

	Vertical	Inclined	Horizontal	Uncertainty
Surface tilt angle β [°]	90	45	0	-
Absolute pressure [bar]	1.28	1.23	1.28	±0.1 %
Saturation temperature [°C]	107	106	107	±0.5
Coolant inlet temperature [°C]	50	50	50	±0.05
Avg. inlet vapor velocity [m s^{-1}]	3.4 – 13.6	3.5 – 13.7	3.3 – 13.8	±0.2

3. Results and Discussions

The departing radius r_{max} is an indicator of droplet removal efficiency during DWC: the larger the departing radius, the lower the efficiency of droplet removal. Moreover, as well established in the literature, r_{max} is a key parameter in DWC heat transfer modeling [5]. Therefore, in the present study, the authors aim to provide a detailed description of r_{max}, accounting for both surface inclination and vapor velocity effects. The departing radius is the outcome of a balance between the adhesion force and external forces. Usually, only the gravity force is considered as external contribution. Nevertheless,

Tancon et al. [8] presented a comprehensive model accounting for the tilt angle of the surface (β) and the additional external force due to vapor drag. The equations of the model are recalled below:

$$r_{max} = \frac{-C + \sqrt{C^2 + 4AB}}{2B} \quad \text{for } 0° < \beta \leq 90° \qquad ; \qquad r_{max} = \frac{A}{C} \quad \text{for } \beta = 0° \tag{5}$$

$$A = 2\, k_c \sin\theta_e\, \sigma\, (\cos\theta_r - \cos\theta_a)$$

$$B = \frac{1}{3}(2 - 3\cos\theta_e - \cos^3\theta_e)\, \pi\, \rho_l\, g \sin\beta$$

$$C = \frac{1}{2}\, \rho_v\, v_{vap}^2\, C_d\, (\theta_e - \sin\theta_e \cos\theta_e)$$

In the previous equations, parameter A accounts for the effect of adhesion force, parameter B for the gravity effect, and parameter C accounts for the drag effect. Further details are given in [5,8].

Figure 2a shows the evolution of the detected departing radii as a function of the average vapor velocity, for all the tested specimens. Regarding P7M3 samples, at the lowest v_{vap} (~ 3 m s^{-1}), the departing radius for the vertical configuration is found to be 1.2 mm (figure 2c), while for the 45° inclined and horizontal configurations, the average r_{max} is about 1.8 mm and 7.9 mm (figure 2b), respectively. In the case of a vertical condensing surface, the direction of the gravity force facilitates condensate removal, maintaining a small average drop size despite the low effect of steam drag. By changing the inclination of the test section, the contribution of gravity to droplet removal is progressively reduced and, at low steam velocity, the average droplet size increases reaching a maximum in the horizontal configuration. The latter represents a critical case since the gravity direction is perpendicular to the droplets motion. It was intriguing to observe that, in the horizontal configuration, even a slight drag effect is sufficient to promote condensate removal, preventing flooding of the surface and transition to filmwise condensation. Increasing the steam velocity resulted in a general decrease in drop size and an improvement in condensate removal for all the three configurations. The most noteworthy result occurred at the maximum velocity (~ 14 m s^{-1}). In particular, reductions in r_{max} of approximately 45% and 80% were observed for the 45° inclined and horizontal configurations, respectively. At the highest velocity, similar values of r_{max} were observed for all configurations (figure 2a). This is a crucial finding, suggesting that, at relatively high velocities, drag effect becomes dominant and is able to compensate the reduction in the gravity force component as surface inclination changes from vertical to horizontal.

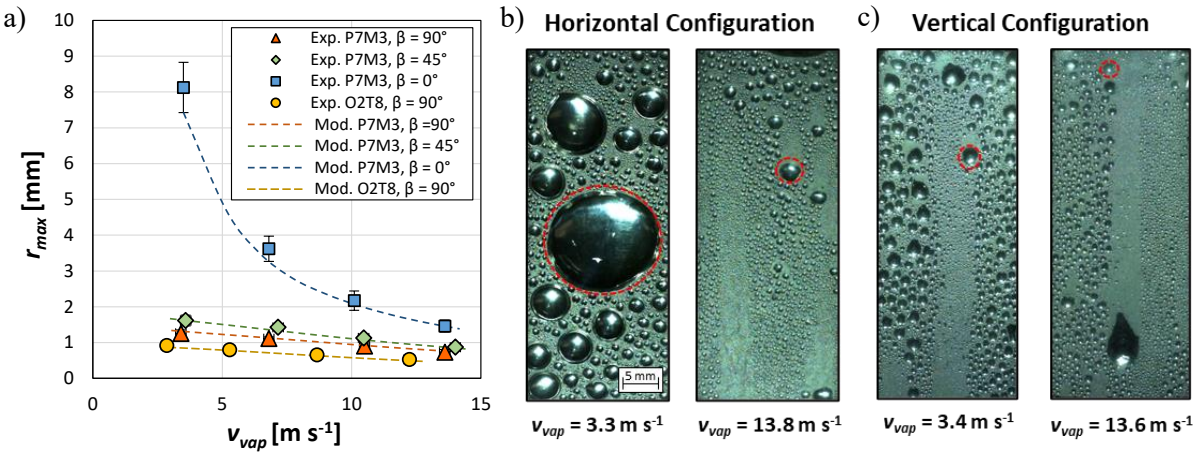

Figure 2. a) Experimental (dots) and predicted (dotted line) droplet departing radius (r_{max}) against vapor velocity (v_{vap}) for the P7M3 and O2T8 samples. b) and c) Experimental visualization of DWC occurring on horizontally and vertically oriented P7M3 sample at two different vapor velocities.

In figure 2a, it is also possible to observe the evolution of the departing radii for the case of the vertically-oriented O2T8 sample. This data set was included in the study to evaluate the ability of the departing radius model (equation 5) to predict the effect of surface wettability on r_{max} and consequently on HTCs. This specimen exhibited lower departing radii compared to those observed for P7M3 sample

tested in similar operating conditions. In particular, at the lowest vapor velocity, r_{max} was almost equal to 0.9 mm and this is mostly related to its higher hydrophobicity. With an augmentation in vapor velocity from 2.8 m s^{-1} to 12.2 m s^{-1}, a 40% reduction in the average departing radius was detected (r_{max} = 0.53 mm). It is possible to conclude that, considering similar operating conditions, P7M3 and O2T8 showed comparable reduction in terms of r_{max} when the vapor velocity increases. In Figure 2a, a comparison between experimental data and model predictions (Tancon et al. [8]) is also presented: it is possible to observe an excellent agreement with a mean deviation lower than 4%. It must be noted that, for all the configurations, the average inlet-outlet vapor velocity has been used as input for the model. This choice arises from experimental findings (figure 2b) which indicate that for $\beta = 0°$ droplets start to slide along the surface from the central region of the sample rather than from the top part.

In addition to the droplet departing radius, heat transfer measurements were conducted in all the three configurations, varying the steam velocity. As depicted in figure 3a, at the lowest v_{vap}, the HTCs obtained for the 45° inclined and horizontal configurations are 10% and 40% lower compared to those measured in vertical configuration (HTC = 97 kW m^{-2} K^{-1}). This trend is compatible with the behavior of the departing radii discussed earlier (figure 2a). Indeed, at low steam velocities, moving from the vertical orientation to the horizontal one, the average droplet size increases, thus resulting in higher thermal resistances. Increasing the steam velocity leads to higher HTCs for all the configurations. At the maximum tested velocity, the three configurations converge to approximately the same HTC value (120 kW m^{-2} K^{-1}). Consequently, steam drag action at such speeds proves to be an effective mechanism for condensate removal able to guarantee high DWC performances also in the case of horizontally oriented surfaces. Heat transfer measurements have been performed also for a vertically oriented O2T8 sample. Results showed HTCs 16% higher than those detected for P7M3 in similar operating conditions (~97 kW m^{-2} K^{-1}). These is related to the lower average drop size observed for O2T8 samples and the lower thickness characterizing this coating (200 nm for 02T8, 400 nm for P7M3). In figure 3a, experimental data have been compared with the predictions from a calculation method obtained incorporating the previously discussed departing radius model (equation 5) into the formulation of heat flux during DWC [5]. It can be observed that the model accurately predicts the increase in HTC with rising velocity for both the vertical and 45° inclined configurations. For the horizontal configuration, larger deviations are observed at the highest vapor velocity. In figure 3b, the mean deviation between measurements and model prediction is reported. Overall, the proposed calculation method provided an accurate prediction of the effects of vapor velocity and surface inclination on the HTC, with a minimum relative deviation of 3% and a maximum relative deviation of 14%.

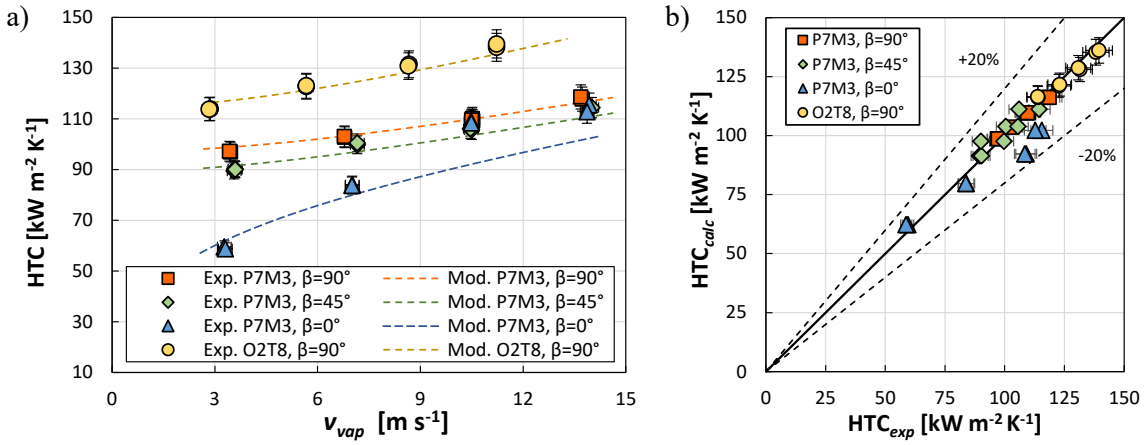

Figure 3. a) Experimental and calculated (dotted lines) HTCs against vapor velocity at different surface inclinations b) Comparison between experimental and calculated HTCs values.

4. Conclusions

Condensation tests were conducted on aluminum samples (functionalized with two coatings named P7M3 and O2T8) showing different surface wettability. The investigated parameters included the droplet departing radius (r_{max}) and the heat transfer coefficient (HTC). Measurements were performed varying the steam velocity (3.3-13.8 m s^{-1}) and, in the case of P7M3 samples, changing the surface inclination (vertical, 45° inclined, and horizontal). At low velocity conditions (~3 m s^{-1}), a departing radius equal to 1.26 mm and 0.92 mm were observed for the vertically oriented P7M3 and O2T8 samples: the departing radius reduction is related to the higher hydrophobicity characterizing O2T8 coating. By progressively reducing the surface inclination, the average drop sizes increase and, in the horizontal configuration, a departing radius equal to 8.1 mm was measured. Interestingly, despite the absence of gravity contribution to condensate removal, the vapor drag effect was sufficient to prevent the transition to filmwise condensation. Increasing the vapor velocity, all configurations showed a reduction of the departing radius: in particular, when the vapor velocity is varied in the range 3-14 m s^{-1}, a reduction of 45% and 80% was observed for the 45° inclined and horizontal configurations respectively. The detected trends for droplet departing radius can explain the HTC variations observed during the experimental campaign run at different vapor velocities and sample inclinations. For the P7M3 sample, at the lowest vapor velocity, the highest HTC was measured in the case of the vertically oriented surface (97 kW m^2 K^{-1}) which displays also the minimum droplet departing radius. Under similar operating conditions, for the O2T8 sample, the heat transfer coefficient was equal to 113 kW m^2 K^{-1}: the HTC increase compared to P7M3 sample is due to the smaller coating thickness and to the wettability characteristics of O2T8 sample. Increasing the vapor velocity, all configurations showed an increase in HTC until reaching the maximum velocity (~14 m s^{-1}) where they reached similar HTC values (120 kW m^{-2} K^{-1}). Finally, the HTC measurements have been compared against a homemade calculation method which is able to account for both the effects of surface inclination and vapor velocity. The proposed method was found to provide accurate predictions.

Acknowledgments

Financial support of European Union - Next Generation EU and Italian Ministry for University and Research (MUR) through the project PRIN 2022 (2022PSPA8R) WADERE is gratefully acknowledged.

References

[1] Khandekar S and Muralidhar K 2020, *Drop Dynamics and Dropwise Condensation on Textured Surfaces* Springer Cham Swizzerland
[2] Mirafiori M, Tancon M, Bortolin S, Martucci A and Del Col D 2022 *J. Phys.: Conf. Ser.* **2177** 012046
[3] Tancon M, Mirafiori M, Bortolin S, Parin R, Colusso E, Martucci A and Del Col D 2022 *Exp. Therm. Fluid Sci*. **136** 110677
[4] Basso M, Colusso E, Tancon M, Bortolin S, Mirafiori M, Guglielmi M, Del Col D and Martucci A 2023 *J. Non-Cryst. Solids X* **17** 100143
[5] Tancon M, Mirafiori M, Bortolin S, Basso M, Colusso E and Del Col D 2022 *Appl. Therm. Eng*. **216** 119021
[6] Citakoglu E and Rose J W 1969 I*nt. J. Heat Mass Tran.* **12** 645-650
[7] Mancio Reis F M, Lavielle P and Miscevic M 2017 *Heat Transfer Eng.* **38** 377-385
[8] Tancon M, Abbatecola A, Mirafiori M, Bortolin S, Colusso E, Martucci A and Del Col D 2024 *Int. J. Therm. Sci.* **196** 108738
[9] Parin R, Tancon M, Mirafiori M, Bortolin S, Moro L, Zago L, Carraro F, Martucci A and Del Col D 2020 *Appl. Therm. Eng*. **179** 115718